Relaxation Behavior of Dense Suspensions

by

Andrew Herman Griese

Submitted to the
Department of Mechanical Engineering
in Partial Fulfillment of the Requirements for the Degree of

Bachelor of Science

at the

Massachusetts Institute of Technology

May 2020

Signature of Author .....
Department of Mechanical Engineering
May 8, 2020

Certified by .....
Dr. Irmgard Bischofberger
Esther & Harold E. Edgerton
Career Development Professor
Thesis Supervisor

Accepted by .....
Dr. Maria Yang
Professor of Mechanical Engineering

Relaxation Behavior of Dense Suspensions

by

Andrew Herman Griese

Submitted to the Department of Mechanical Engineering
on May 8, 2020 in Partial fulfillment of the
requirements for the Degree of Bachelor of Science
in Mechanical Engineering

ABSTRACT

Dense suspensions of solid particles in Newtonian fluids exhibit a variety of non-Newtonian behaviors depending on the shear stress applied to the suspension and the particle mass fraction (ϕ_m). Suspensions at sufficiently high ϕ_m shear-thicken dramatically and eventually shear jam, showing behaviors typified by solids. But, little is known about how dense suspensions relax out of this stressed rheological state. To understand the relaxation behavior of a cornstarch/water dense suspension, samples are prepared at different ϕ_m, in the range that shows dramatic shear thickening, between 54.5% and 58.5% cornstarch. Each sample is formed into drops and kept in the stressed state through dynamic shearing using a B&K permanent magnet shaker, then allowed to relax. We show that dense suspensions relax with two distinct timescales. A short timescale that is independent of ϕ_m, denoting the settling of the drop onto the flat surface, and a longer timescale that is governed by the viscosity of the dense suspension and increases as ϕ_m increases above 55.75%. Our work provides an understanding of how a dense suspension relaxes out of a shear-thickened state.

Thesis Supervisor: Irmgard Bischofberger

Title: Esther & Harold E. Edgerton Career Development Professor

1. Introduction

The phenomenon of shear thickening in dense suspensions defies one's intuition. A suspension of cornstarch particles and water (commonly termed Oobleck), if mixed in the right mass fraction (ϕ_m), is the most prominent example of a strongly shear-thickening material and is used in elementary school classrooms across America to inspire students' curiosity. The awe it rouses by playing with the material or even running on it is due to the complex rheological behavior of dense suspensions: they can exhibit both liquid-like and solid-like properties depending on the stress applied to the material.

An understanding of the mechanism behind this complex behavior has only recently started to emerge. It has been shown that dense suspensions are characterized by a number rheological properties: they are yield-stress materials – flowing only at stresses above a critical stress – and exhibit both discontinuous shear-thickening (DST) and shear-jamming (SJ) behavior as a response to an applied stress. The best way to visualize these different states is through rheology data. Figure 1 illustrates the three distinct trends of the viscosity response of a shear thickening dense suspension to a changing shear stress [2]. After the yield stress is reached (dashed line in Fig. 1) the dense suspension begins to flow. As stress is increased, the suspension begins shear thinning where particles not in contact move past each other easier and easier (blue region in Fig. 1) [2], until the viscosity reaches a minimum and the suspension behaves similar to a Newtonian fluid characterized by an almost stress-independent viscosity (red region in Fig. 1). Upon a further increase in stress, the particles become more tightly packed and begin to create frictional contacts leading to a linear increase of the viscosity with stress (green region in Fig. 1) [2]. This region is what is termed DST.

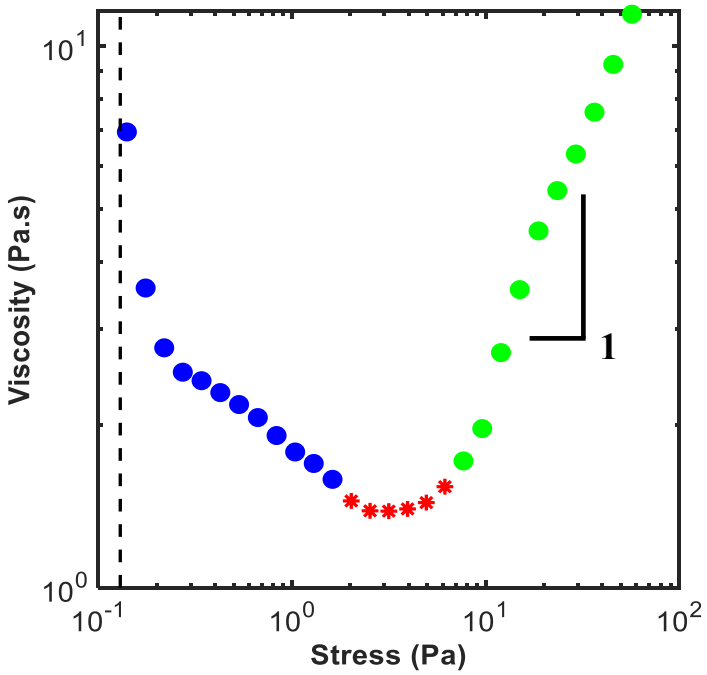

Figure 1: Rheological response of a 56% mass cornstarch and water dense suspension to an applied stress. Unlike Newtonian fluids, dense suspensions exhibit three distinct states when an increasing shear stress is applied. Dense suspensions are yield stress fluids; they only flow above a critical stress, called the yield stress, indicated by the dashed vertical line. In the blue region the suspension exhibits shear thinning behavior, where the viscosity decreases with increasing stress. In the red region the suspension behaves similar to a Newtonian fluid where the viscosity is practically constant with increasing stress. Lastly, the suspension shear thickens in the green region where increasing the shear stress leads to an increase in the viscosity. This shear thickening region is responsible for the unique behavior of dense suspensions.

Discontinuous shear-thickening describes the strong increase in a fluid's viscosity as the applied stress increases. Shear-jamming is a transition into a solid-like state, characterized by the appearance of a second critical stress below which the material does not move. Extensive experimental, numerical, and theoretical research on the rheology of dense suspensions has recently established the shear stress, rather than the shear

rate, as the key control parameter for the state of the suspension [3,5,6]. In particular, it has been shown that rate-controlled experiments preclude the investigation of the steady-state DST regime, which is accessible only at a range of specific stresses; this is because the shear rate exhibits a discontinuous transition, while as the stress increases viscosity increases continuously. While rate-controlled experiments can determine the onset of DST, the full DST regime and in particular the SJ regime can only be probed by controlling the stress. The macroscopic behavior of shear thickening is the result of complex microscopic interactions. Shear thickening is the result of inter-granular repulsion and results from the dilation of the suspension [1]. When a weak shear stress is applied the grains in the suspension slide past each other with little resistance [1]. But if the shear stress is higher the inter-granular friction increases dramatically which can lead to an increase in dilation of the grains as well [1]. Suspensions with high enough ϕ_m of particles exhibit the rheological states shown in Figure 1. With increasing ϕ_m, the minimum viscosity (red region in Fig. 1) increases, as shown in Figure 2.

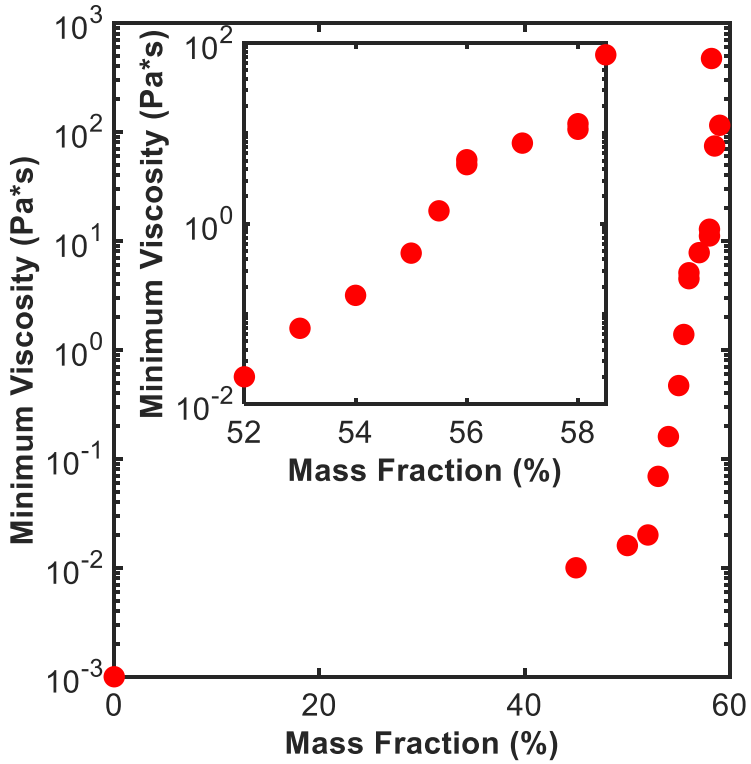

Figure 2: The viscosity of dense suspensions with varying cornstarch concentration ϕ_m. The minimum viscosity, corresponding to the stress independent regime, increases as the cornstarch concentration ϕ_m increases. The inset is the range of cornstarch concentration ϕ_m that is applicable to this experiment. Over this range of interest, the minimum viscosity increases by two orders of magnitude.

The fascinating behavior of shear thickening dense suspension is not just a science class phenomenon. It can be used to potentially save lives. Kevlar when impregnated with a silica shear thickening fluid had improved projectile energy absorption compared to unaltered Kevlar [7]. This is believed to be due to the shear thickening on impact adding to the force required to pull the Kevlar threads past one another [7]. With more understanding of dense suspensions when they are shear thickening and when they are at rest could lead to improved ballistic body armor. Dense suspension liquid like equilibrium state could allow for body armor that fits the body's contours better allowing for more coverage and greater comfort while not sacrificing protection with its shear thickening properties.

Such potential applications, however, cannot happen until the field gains a more complete understanding of dense suspensions. Previous work in the field has largely focused on the shear thickening property, and almost all of that work has looked into one side of the phenomenon: The papers cited here [1-7] and countless more focus on the mechanics and behavior of how a dense suspension gets into a certain

rheology state. The research has evolved from understanding the mechanics of the phenomenon [2] to developing a robust constitutive model for DST [1]. This study focuses on how a dense suspension sample vibrated at high enough frequency to cause large enough shear stress to "lock" the sample in its solid-like state relaxes to a state where such dynamic perturbation is removed. We show that cornstarch and water dense suspensions relax out of a shear thickened state through a two-timescale exponential relaxation.

2. Experimental Methods

To gain a better understanding of the relaxation behavior of cornstarch/water dense suspensions, we investigate samples at varying ϕ_m of cornstarch, ranging from 54.5% cornstarch to 58.5% cornstarch. This range is chosen specifically for that the suspension maintains its shape as a ball during the experiment and that it could be mixed to a homogenous mixture (verified by visual and touch inspection) using a spoon and hand kneading. Below ϕ_m = 54.5% the viscosity of the dense suspension is too low to form a ball and the sample flows. Above ϕ_m = 58.5% the dense suspension is impossible to homogeneously mix. The six cornstarch mass fractions used throughout testing are ϕ_m = 54.5%, 55.75%, 57%, 57.5%, 58%, and 58.5%.

Samples are prepared by first calculating the mass of cornstarch needed for a suspension of specific ϕ_m, keeping the volume of water constant at 50 ml. A clean plastic mixing bowl is placed on an electronic scale (accurate to 0.01g), zeroing the scale on the bowl to minimize confusion. The desired amount of cornstarch and 50 ml of water are poured into the bowl consecutively. These components are mixed at first with a plastic spoon and then kneaded liked bread by nitrite gloved hands until the suspension feels and looks homogenous. For the purpose of studying the effects of the background fluid viscosity, some samples were made by adding glycerol to the suspension to increase the viscosity, similarly to the study by Dr. Peters et al (2016). The same mixing process is followed for the glycerol water and cornstarch dense suspensions, the only variation is that glycerol and water are mixed before being poured onto to the cornstarch. Each of these samples is only used for three trials performed within a time window of 5-10 minutes to ensure they do not dry out during use and change ϕ_m.

The experimental setup, shown in Figure 3, allows for a precise control of the start time, an unobstructed view of the relaxation of the dense suspension over time, and easy cleaning/setup for repeated trials. Precise control over the start of the experiment is obtained through the use of the B&K V203 permanent magnet shaker, which when operated at a 40 Hz sine wave with an amplitude of 7.2 volts keeps the sample bouncing in a stressed state until it is turned off. A screw on laser cut acrylic platform allows for an unobstructed view and easy setup. Two FLIR Grasshopper3 cameras synchronized with FlyCapture2 SDK software capturing at 9 frames per second are used for data collection.

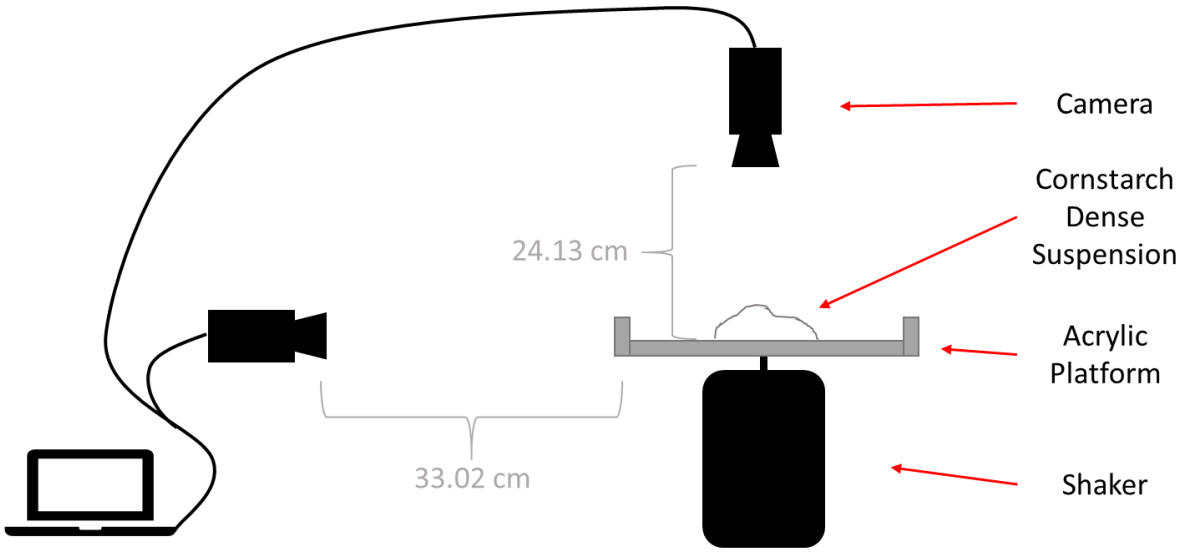

Figure 3: The experiments base is a B&K V203 permanent magnet shaker with an input of a 40 Hz sine wave with an amplitude of 7.2 volts. This input is found through trial and error but ensured the suspension remained excited until t=0. The cornstarch dense suspension is dropped onto a 0.127 m x 0.127 m acrylic platform with the underside painted black to allow the white sample to stand out. The experiment is capture using two FLIR Grasshopper3 cameras synchronized with FlyCapture2 SDK software at 9 frames per second.

To investigate the relaxation behavior of the suspensions, 8-11 ml of the material is scooped out of the plastic bowl with a spoon. Using a gloved hand, the suspension is formed into a ball and placed on the center of the shaker. The shaker keeps the sample in a stressed state with a quasi-ball shape. After a few seconds of bouncing the shaker is turned off at t=0 and the relaxation behavior of the sample is imaged. To quantify this relaxation of the dense suspensions with different ϕ_m, we calculate the area of the drop for each time step, as shown in Figure 4 for the area at t=0 and the final area.

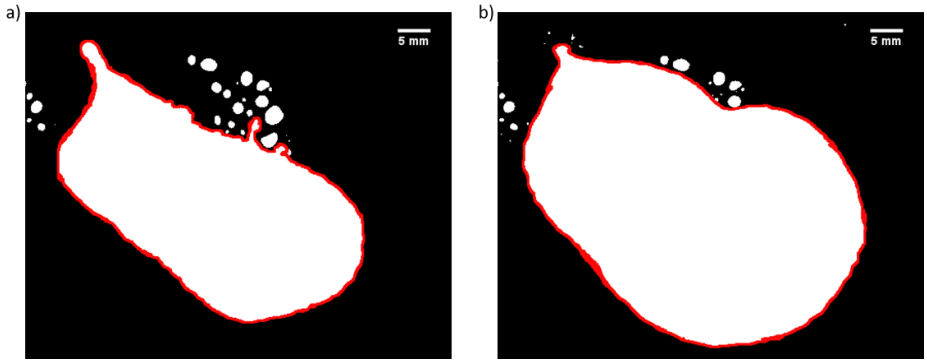

Figure 4: The visualization of drop areas, to be used in later analysis of data. Image a) and b) are the binarized photographs collected during the experiment by the vertical FLIR Grasshopper3. They represent the areas a_0 (time t = 0) and a_f (end of experiment) respectively. The red outlines represent the area calculated at each time.

The spreading behavior exhibits large variations for the range of cornstarch concentrations ϕ_m investigated. To compare the relaxation behavior of different ϕ_m and of drops of different initial sizes, we consider the change in area over time normalized by the total change in area, expressed as $A(t)=(a_f-a(t))/(a_f-a_0)$, where a_f is the final area at the end of the spreading and a_0 is the initial area at t=0. t=0 corresponds to when the shaker is turned off and the drop impacts the platform. t=final corresponds to the end of the experiment when the drop is no longer is visually spreading ~15-20s after t=0.

The percent area change data exhibits a double exponential decay, Equation (1), which suggests two distinct relaxation processes.

$$A(t) = \mathrm{B} * \mathrm{e}^{-\frac{t}{\tau_1}} + (1 - \mathrm{B}) * \mathrm{e}^{-\frac{t}{\tau_2}} \quad (1)$$

In addition to quantifying the radial expansion of the drop, our two-camera synchronized setup allows us to examine the relaxation behavior of the side profile of the sample. Figure 5 describes how we first, similar to the area, have to take the raw tiff images and turn them into quantitative data. Since the side profile has complex shadows and cannot be binarized, the outlining is done by hand (yellow outline Fig. 5 a). This outline is a good representation of the side profile with an error of a few pixels due to user imprecision. This outline is then filled and the background cleared to allow for the plot profile tool to determine the average height (Fig. 5 b).

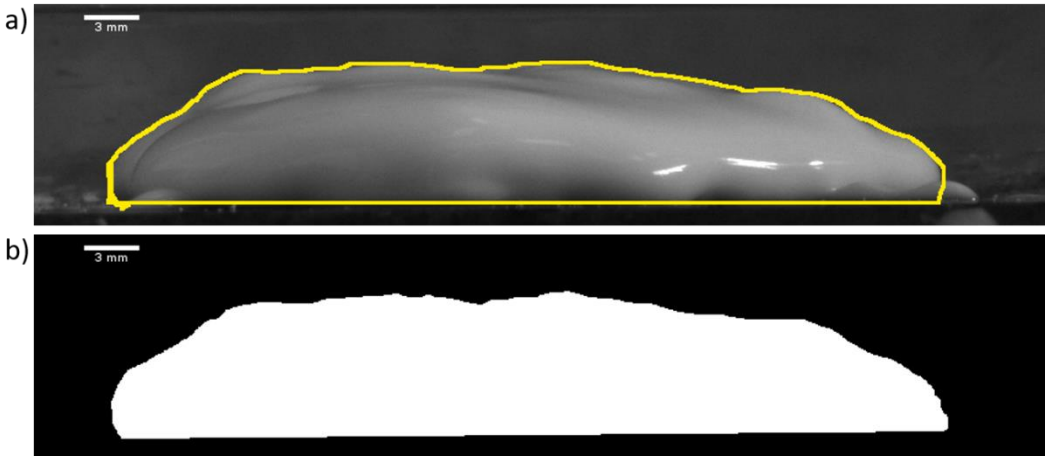

Figure 5: The process to measure the side profile average height of the drop at a given time. Photograph a) shows a ϕ_m =55.75% drop at t=τ_2 outlined using ImageJ. Photograph b) is the same image cropped to size with the background cleared and the outlined side profile filled with white. The image in b) is then cropped and exported to excel using the plot profile tool and the pixel height is averaged over the length of the drop.

While there are many advantages to the experimental setup, some potential causes for error include: due to the randomness of the bouncing ball, the sample is not always the same distance from the side camera. There is ~1.5 mm change in scale from the front edge of the platform to the rear edge. This is small compared to the side profile measurements but should be noted. Also, the limited frame rate and fast changes occurring near τ_1 make it almost impossible to have an image at exactly τ_1. But, by τ_2 the drop is in a quasi-equilibrium state so being up to 0.06 s off is acceptable, making this type of measurement only useful for τ_2. When bouncing before the shaker is turned off at t=0, the sample would often leave little droplets behind. This leads to discontinuities in some of the area measurements, as the area changes when a droplet is absorbed. Lastly, due to the limitations in mixing and ball formation, experiments are only conducted in a limited range of ϕ_m compared to that tested in rheology. These potential errors should be noted but still allow for useful data collection. For example, even with some imprecision the side profile height is still an important measurement in our understanding of relaxation, it shows up in the rescaling for estimated viscosity late in the paper and helps us determine what sets the final size of the drop.

3. Results and Discussion

The progression of the experiment once the sample is in the stressed state is captured in Figure 6. The area of the drop as imaged from above changes drastically over the course of the experiment. The drop spreads out on the plate radially as time increases until it reaches a final size in (6e top image). The relaxation is further observed from the side, where the stressed sample impacts the plate then begins to thin and expand horizontally. Immediately following impact (6b & 6c) the drop seems to settle on onto the platform with little radial expansion. But from the side we see the drop fill in the ridges are not in contact with the platform on impact by 6c. The side view also appears to show the drop reaching a final state.

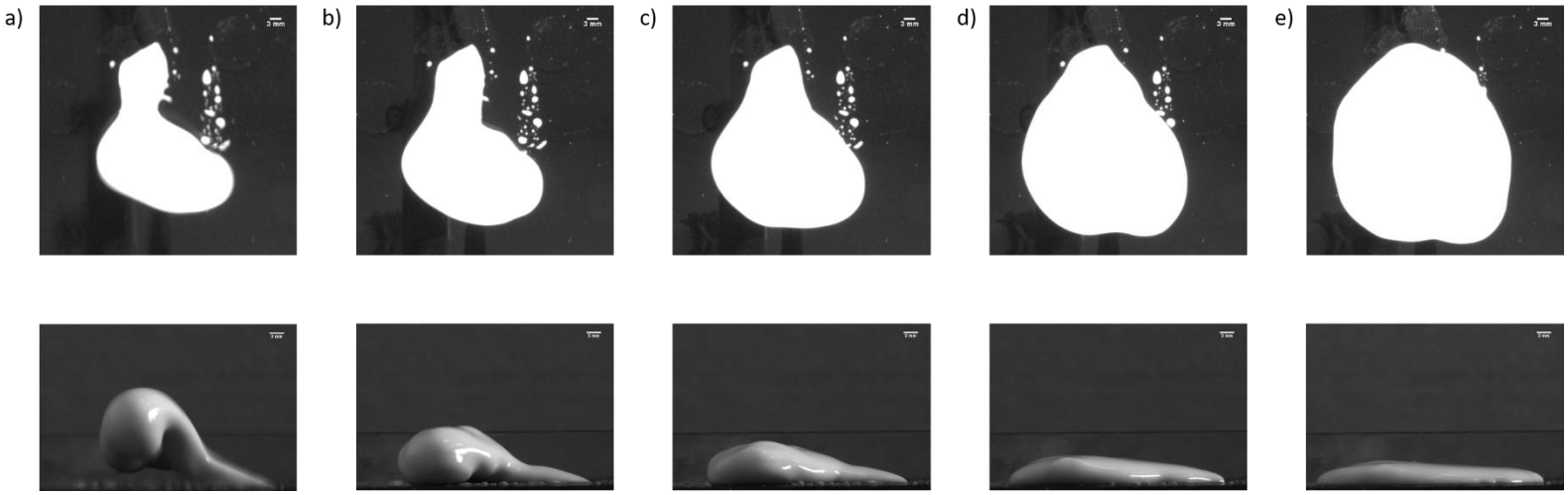

Figure 6: One trial of ϕ_m = 55.75% from side (bottom) and top (top) view. Time increases from left to right with a) before t=-0.x s, b) t=0 s, c) t=0.2 s, d) t=0.78 s, e) t=4.0 s. The sample in a) is bouncing in a quasi-ball shape before the start of the experiment while the shaker is on. After t=0, notice the drastic changes in height and area during the first second of relaxation, b) to d).

$A(t)$ decreases with time, indicating the spreading of the suspension, as shown in Fig. 7(a) for three different ϕ_m. As ϕ_m increases (black to blue to red) the drop spreads slower. This is shown by the decrease in slope as the ϕ_m increases because the area changes less per time step. Equation (1) describes the normalized area well. It maintains a close fit until the previously discussed discontinuities disrupt the data, as the sample absorbs other droplets. To understand the parameters that govern the relaxation, we further vary the solvent viscosity by replacing the water with a glycerol/water mixture that has a viscosity of 20x that of water. Increasing the solvent viscosity leads to slowing down the drop's spreading because the suspensions viscosity increases with the solvent viscosity. This equates to how a drop of honey spreads much slower than a drop of water. As shown in Figure 7(b) the glycerol/water suspension (open circles) has a much slower relaxation than the water suspension (closed circles).

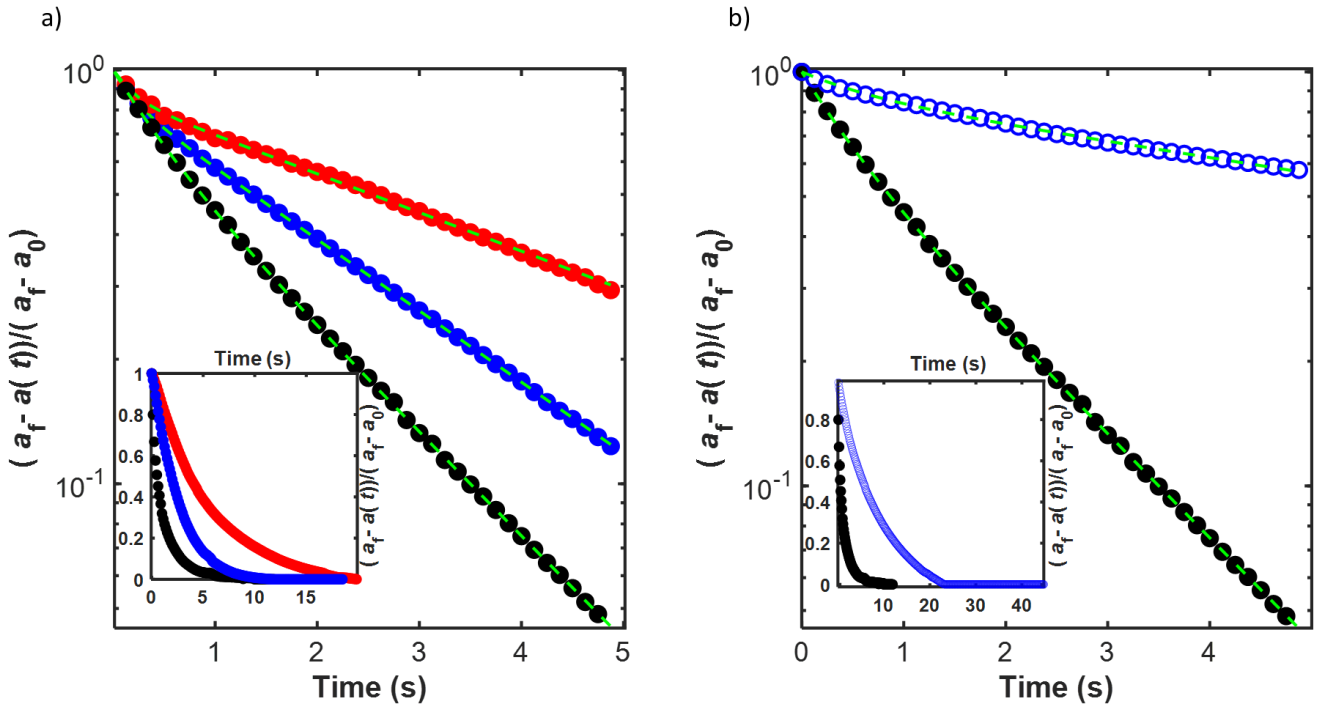

Figure 7: Temporal evolution of the drop area. a) representative trial at ϕ_m = 54.5% (black), 57% (blue), and 58.5% (red), with each trial's fit of Equation (1) overlayed in green. b) comparison between the relaxation of ϕ_m =54.5% in a water/glycerol mixture (blue) and in water (black). The inset shows the same data with both linear axes.

The data clearly shows variation in the behavior as the ϕ_m changes. The nontrivial double exponential fit of Equation (1) leaves us with two distinct time scales for each ϕ_m. This raises some important questions about how the cornstarch dense suspension relaxes. What governs these two timescales? What do they represent?

First, we explore how the drops of different ϕ_m qualitatively change throughout the experiment. Figure 8 shows the relaxation at key times; Fig. 8 a) is t=0, Fig. 8 b) is t=τ_1, and Fig. 8 c) is t= τ_2, for ϕ_m = 54.5% (blue), 57% (orange) and 58.5% (gray). As time progresses all the ϕ_m have a similar increase in radial spreading and thinning of the side profile. At t=0, 57% and 58.5% look similar with the drop still maintaining a quasi-ball shape. By contrast, 54.5% has already deformed out of the ball shape (more to be discussed later). By τ_1 all ϕ_m show a slight decrease in side profile height with relatively little radial area change. As the samples reach τ_2 the shape is practically static in a quasi-equilibrium state, but the drops have radially expanded and their side profiles have thinned. At this timescale, lower ϕ_m expand greatly from the initial drop's area and thin to just a sliver. 57% has thinned and expanded noticeably but less than the 54.5% drop. While the 58.5% drop has changed relatively little with some thinning and radial expansion.

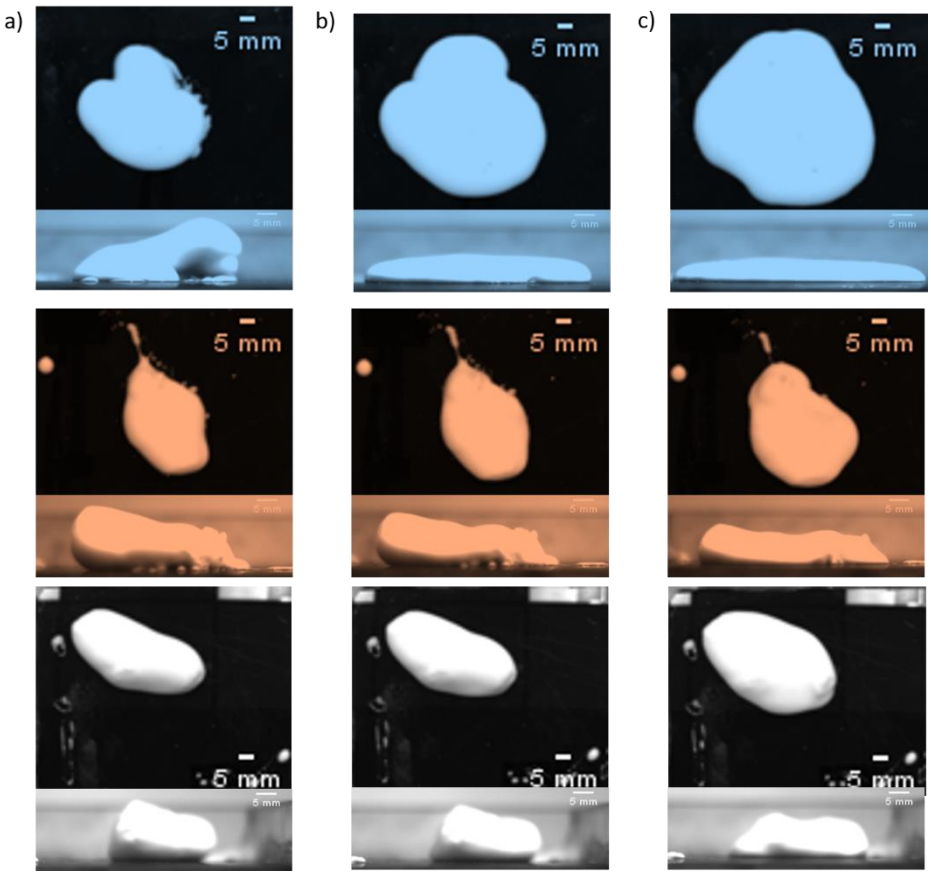

Figure 8: Photographs of key moments in relaxation. The columns represent; a) t=0, b) τ_1, and c) τ_2. The rows differentiate three ϕ_m's of 54.5% (blue), 57% (orange), and 58.5% (gray). The vertical camera view is on top and the horizontal camera is the photographs on the bottom in each image pair. Notice the flattening of the drop from left to right as time increases.

The qualitative analysis shows the differences in these two timescales. τ_1 happens shortly after t=0 and is characterized by a decrease in thickness with no significant change in radial area, except for ϕ_m =54.5% (to be discussed later). τ_2 occurs later and is typified by a substantial decrease in thickness and increase in radial area. Visually τ_2 has a larger variation in thickness and radial area as ϕ_m changes. τ_1 appears to be similar to the time scale studied by Dr. Boyer et al. (2016). This study focused on the momentary equilibrium state found right after impact of a drop of dense suspension on a flat surface [4]. Although the work mainly focuses on this fast time scale ~ τ_1, they do mention observing relaxation after that initial time scale ~τ_2 [4]. This provides important semi-verification of the two timescale fit. To better compare with Boyer's results, we explore τ_1 quantitatively in Figure 9.

The short timescale τ_1, is explored in Figure 9 by first comparing the initial 8-11ml drop experiments with varying ϕ_m (red Fig. 9 a) & b)) to τ_1 of drops with varying size. τ_1 is constant across all ϕ_m and drop sizes, as shown in Fig. 9 a). τ_1 is further constant if the viscosity of the dense suspension is increased by introducing glycerol to the water/cornstarch dense suspension, as shown in Fig. 9 b).

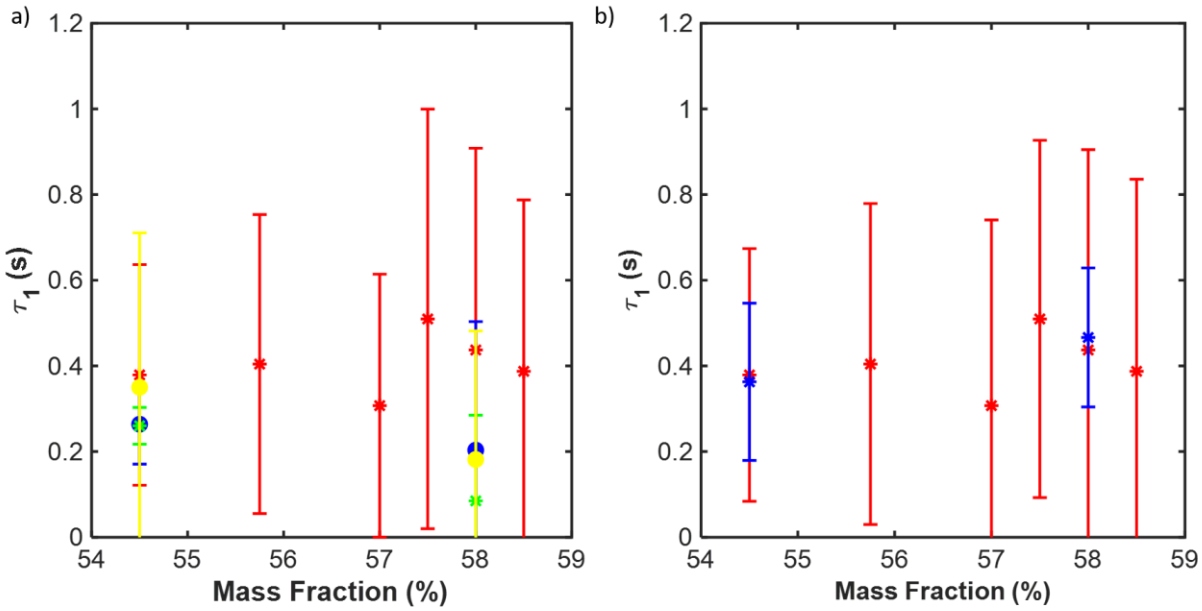

Figure 9: Comparison of τ_1 at different mass fraction. a) τ_1 is independent of drop size for drops of 8-11 ml (red), 8 ml (blue), 2.5 ml (green), 25 ml (yellow), in agreement with Boyer [4]. b) τ_1 is independent of the solvent viscosity, as shown by comparing a cornstarch dense suspension in a glycerol/water mixture with 20x the viscosity of water (blue) and a cornstarch dense suspension in water (red). The large variation in the data is due to the frame rate of the camera being limited to 9 Hz.

Since τ_1 exhibits no statistically significant change as ϕ_m increases it represents a relaxation that is universal across all ϕ_m. Either what occurs does not depend on the properties that vary with ϕ_m (ie: density, viscosity, and distance between particles) or the changes cancel out. To determine what is governing this timescale we add glycerol, similarly to Peters et al. 2016, which increases the background viscosity of the suspension with no undesired chemical effects [2]. The 64% glycerol/water mixture produces a background viscosity of ~ 20 times that of water. Rejamming describes the material compressing as it contacts the platform leading to an increase in shear stress leaving the suspension in it jammed (solid-like) state. If τ_1 is a result of rejamming after impact, we expect that this would lead to large increase in τ_1 due to increasing the viscosity but keeping the density and distance between particles fixed. This reasoning of τ_1 is that it remains constant across all ϕ_m because viscosity distance between particles change at a similar rate. The similar rate leading to cancelation could be thought of as lower ϕ_m means larger inter-particle distance, but lower viscosity means the particles can move faster. So, as ϕ_m increases particle spacing decreases but so does particle speed. However, as seen in Figure 9 b) τ_1 remains constant for the suspension in the glycerol/water mixture. τ_1 therefore represents the settling of the drop onto the flat surface, which is independent of any of the properties, and just represents the drop touching down onto the acrylic platform. This is in agreement with Boyer's findings, which observed that while the deformation after impact depends on the size of the drop, all drops regardless of size show similar behavior immediately following impact [4]. It is important to note that this work used dense suspensions at much lower mass fractions and the drops were dropped from much higher heights. This similar behavior and timescale of deformation is similar to our τ_1.

With τ_1 being independent of ϕ_m we expect τ_2 to show some variation with changing ϕ_m to account for the differences we see in Figure 7 and 8. Additionally, we expect that the viscosity will govern τ_2 to account for the two orders of magnitude change in viscosity in the rheology data (Fig. 2).

The second longer timescale τ_2 varies significantly as the ϕ_m increases, as shown in Fig.10 a) & b) for 8-11ml drops (red). Similarly to τ_1, τ_2 of the water/cornstarch drops is compared to drops of different size (Fig. 10 a)) and to drops of a glycerol/water/cornstarch (blue) suspension (Fig. 10 b) & c)). τ_2 changes greatly with the addition of glycerol. 54.5% and 58%'s τ_2 s increased by ~4x (Fig. 10 b)). These higher data points are related by roughly the same nearly exponential slope as the water/cornstarch suspension is between 55.75% and 58.5%. This indicates that the viscosity governs τ_2; indeed, normalizing τ_2 with the suspension viscosity measured in rheology leads to a roughly constant value (Fig. 10 c)).

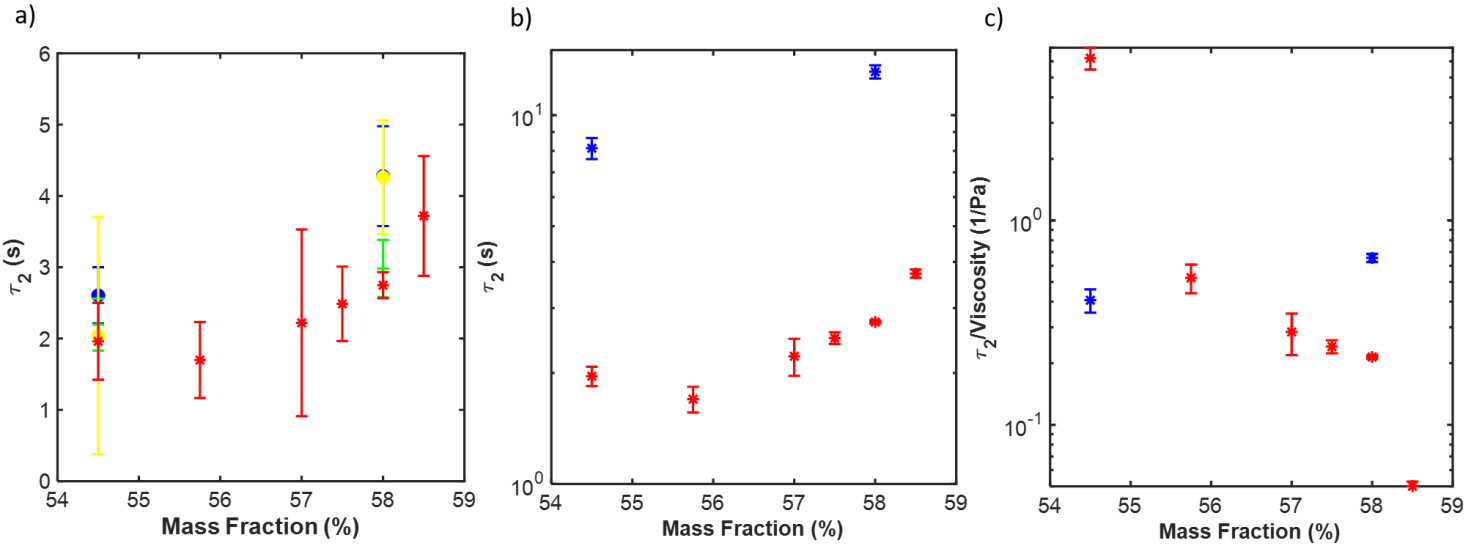

Figure 10: Dependence of τ_2 on ϕ_m. a) τ_2 for drop sizes of 8-11 ml (red), 8 ml (blue), 2.5 ml (green), 25 ml (yellow). b) τ_2 depends on the solvent viscosity as shown by comparing a glycerol water and cornstarch dense suspension with 20x the viscosity (blue) and a cornstarch water dense suspension (red). c) Normalizing τ_2 with the drop's viscosity collapses the data to $\approx 0.3\ \frac{1}{Pa}$.

The second timescale τ_2 increases, as expected, with increasing ϕ_m. This holds true for the mean of each ϕ_m except 54.5% which is longer than 55.75%. The second timescale, unlike the first, is dependent on the viscosity of the dense suspension; when glycerol is added to the cornstarch and water dense suspension, τ_2 increases to 4 times that of the unaltered cornstarch and water dense suspension. The adding of glycerol to the suspension only effects the viscosity therefore confirming that the viscosity is the driving factor behind τ_2 's behavior.

Drop size does not impact τ_1, and it was assumed the same would be true for τ_2 . But, while ϕ_m =54.5% does largely overlap for all drop sizes there is a slight increase. ϕ_m =58% has a consistent increase as all new data shifted upward. The exact reason for this shift is unknown but currently we believe it is due to the slight variation in moisture content of the two cornstarch buckets used. The drop size variation data used a new bucket compared to the original 8-11 ml data. This variation could explain the shift we are seeing but further study will be necessary to confirm this.

To verify our findings, we compare our data to the rheology data by converting the timescale to an effective viscosity. The stress is proportional to viscosity times the shear rate, $\eta * \dot{\gamma}$, and we express the shear rate as shown in Equation (2), accounting for the spreading by using the radial area the diameter's rate of change, $\dot{D}$ and the height h

$$\dot{\gamma} = \frac{\dot{D}}{h} = \frac{D}{\tau_2 h} \tag{2}$$

After τ_2 the sample is in quasi-equilibrium with relatively little change. The only force acting on the spread out sample is then the gravity, which is balanced by the stress times the area of the material since no acceleration is occurring. So at τ_2 we start with Equation (3).

$$\rho Vg = \sigma A \tag{3}$$

Replacing σ with $\eta^*\dot{\gamma}$, plugging in Equation (2), and simplifying gives Equation (4).

$$\frac{\rho h^2 g \tau}{D} = \eta \tag{4}$$

Since the volume is constant, we can rewrite Equation (4) as Equation (5).

$$\eta = \frac{b h_2^{2.5} g \rho}{V^{.5}} \tau_2 \tag{5}$$

Equation 5 relates τ_2 to viscosity using its side profile height h (discussed later), volume V, density ρ, and a correction factor b ~0.32 that is determined by shifting the data on top of the rheology data, as shown in Figure 11. In our concentration range of interest, the minimum viscosity from rheology (red) increases by two orders of magnitude. The estimated viscosity, from Equation (5), for the water/cornstarch drops (blue) and for the glycerol/water/cornstarch drops (green) matches the viscosity from rheology well, particularly in the range of ϕ_m = 55% to 58.5%. As in previous data 54.5% is an outlier and does not rescale properly.

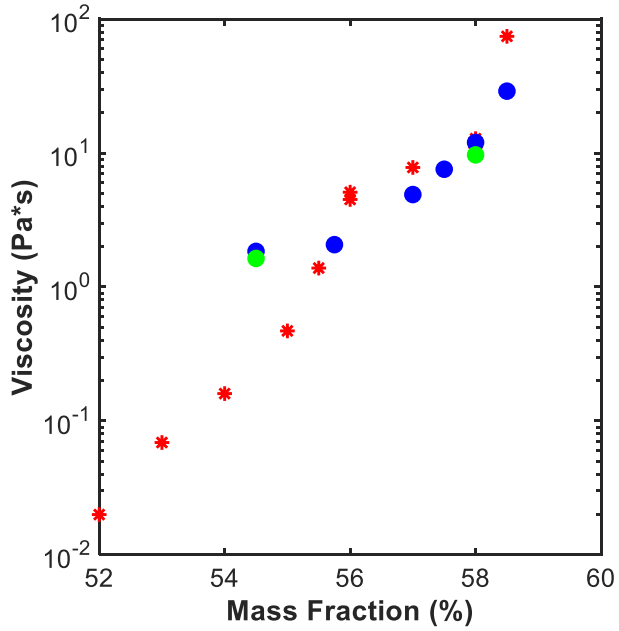

Figure 11: Comparison between the viscosity estimated from τ_2 and the minimum viscosity measured in rheology. The data from both the cornstarch water dense suspension (blue) and the cornstarch water and glycerol dense suspension (green) collapse onto the minimum viscosity from rheology (red). The ϕ_m =54.5% point is an outlier in the data possibly due to premature relaxation before *t*=0 in the experiment.

How well the estimated viscosity from the rescale fits the minimum viscosity of the rheology data emphasizes how important viscosity is to this timescale and provides a sanity check that the findings of this experiment align with the previously taken rheology data. Interestingly, the close agreement at higher concentration with the minimum viscosity points to the relaxation between τ_1 and τ_2 being governed by the Newtonian regime of the dense suspension behavior, as the Newtonian regime defines the minimum viscosity for each ϕ_m.

The unexpected behavior of 54.5% leads us back to the images. Most trials of the 54.5% are already stuck to the acrylic platform before *t*=0, which is seen in Figure 7, where the left side of the sample has already begun to relax at *t*=0. Since some of the sample is not in an excited state at *t*=0 the relaxation we see is different than that of the other ϕ_m. This prestart relaxation is also seen in the 54.5% glycerol/water suspension. The relaxation might explain the different behavior we see in the data and is likely due to 54.5% being the lower bound of our ball formation ϕ_m, which likely needs a different shaker input to remain excited.

So far, the focus of our discussion has been on the area's radial relaxation. The side profile height, however, also has a story to tell. To compare the white and black images discussed in Figure 4 we center and overlay several trials in Figure 12. The whiter the area, the more drops it occurs in. Images a, b, and c are the average drop shapes for ϕ_m =54.5%, 57%, and 58.5%, respectively. As ϕ_m increases, so does the side profile height. We note that the highest and lowest concentrations exhibit lesser variation between trials than the intermediate concentrations. The side profile of the 54.5% drops is long and thin with shallow edges, distinct from the original ball shape, while side profile of the 58.5% drop is round and tall, retaining some of the features of the original ball shape.

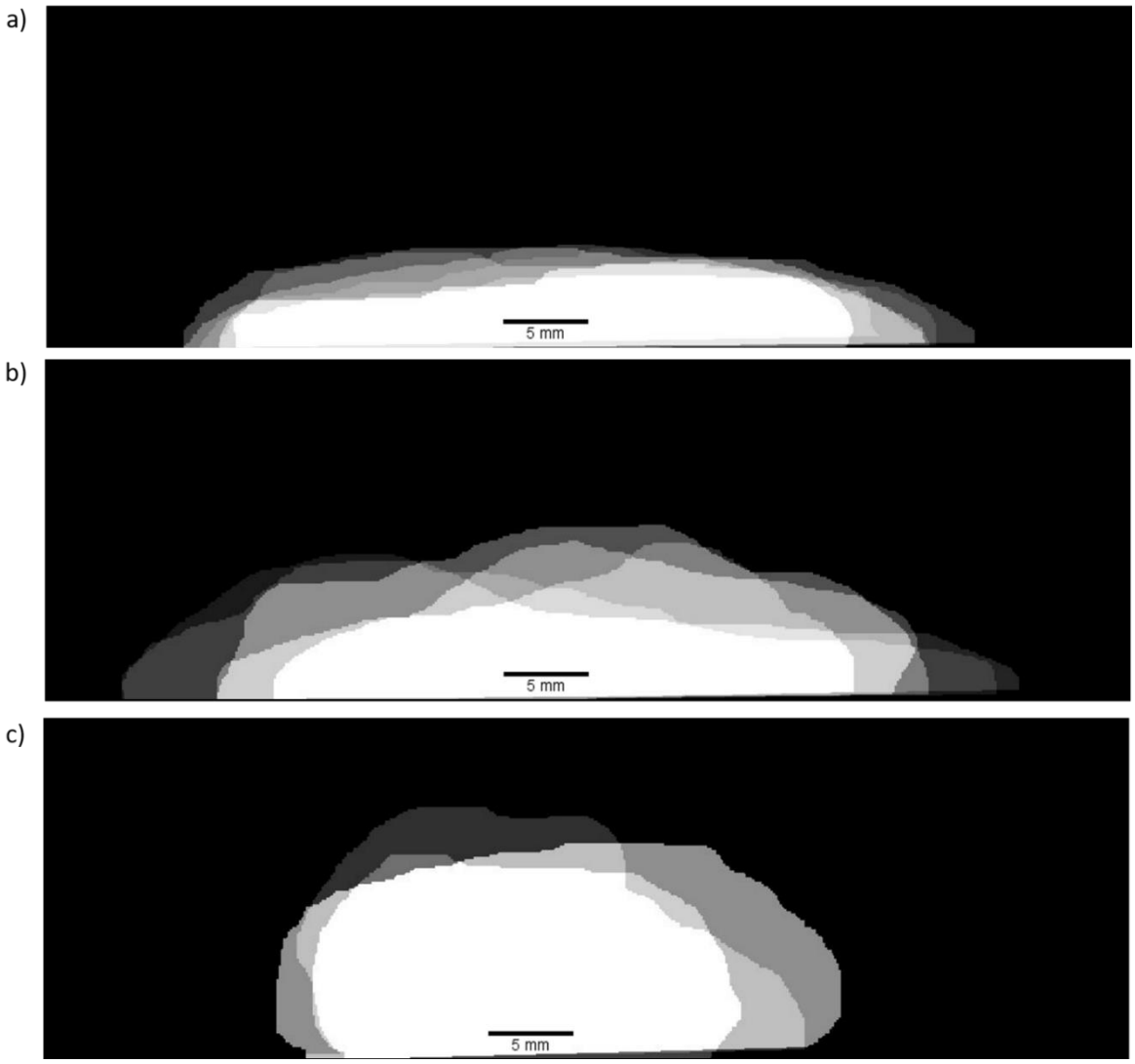

Figure 12: Side profiles of suspensions with ϕ_m =54.5% (a), 57% (b), and 58.5% (c) at τ_2. The height of the side profile increases as ϕ_m increases and the profile maintains its initial circular shape the more the ϕ_m is increased. The images all have the same scale.

At lower ϕ_m, 54.5% and 55.75%, the sample spreads out more and becomes thinner similar to the shape of a pancake. At the highest ϕ_m, 58% and 58.5%, the sample retains its ball like shape with steep edges and with little radial spreading. At intermediate concentrations, 57% and 57.5%, the sample has a shape that combines the two; some trials spread out more, others remain closer to a ball, some do some of both.

The variation of profile and height brings to question why these samples stop spreading; why do they not spread like water until the cover the whole platform? At equilibrium when the drop has stopped spreading the normal stress of the suspension times the area is equal to the force from gravity. The shear

stress of the suspension, naturally, is expected to scale as this normal stress. Due to dense suspensions being a yield-stress material the spreading ceases once the suspensions stress reaches the yield stress σ_y, because below the yield stress the suspension will not flow. This equilibrium yields Equation (6).

$$\frac{\sigma_y}{\rho g} = h \tag{6}$$

Equation (6) again allows us to compare our data to the yield stress measured in rheology (in Fig. 13. a)). Notice the near tenfold increase in yield stress as ϕ_m increases from 56% to 59%. We use equation (6) to estimate the side profile height from the rheology yield stresses and compare it to the side profile heights measured at τ_2, as shown in Fig. 13 b) where we report the height at τ_2 estimated from the yield stress (blue) and the side profile height (red). They exhibit a similar dependence on the cornstarch concentration but are shifted numerically.

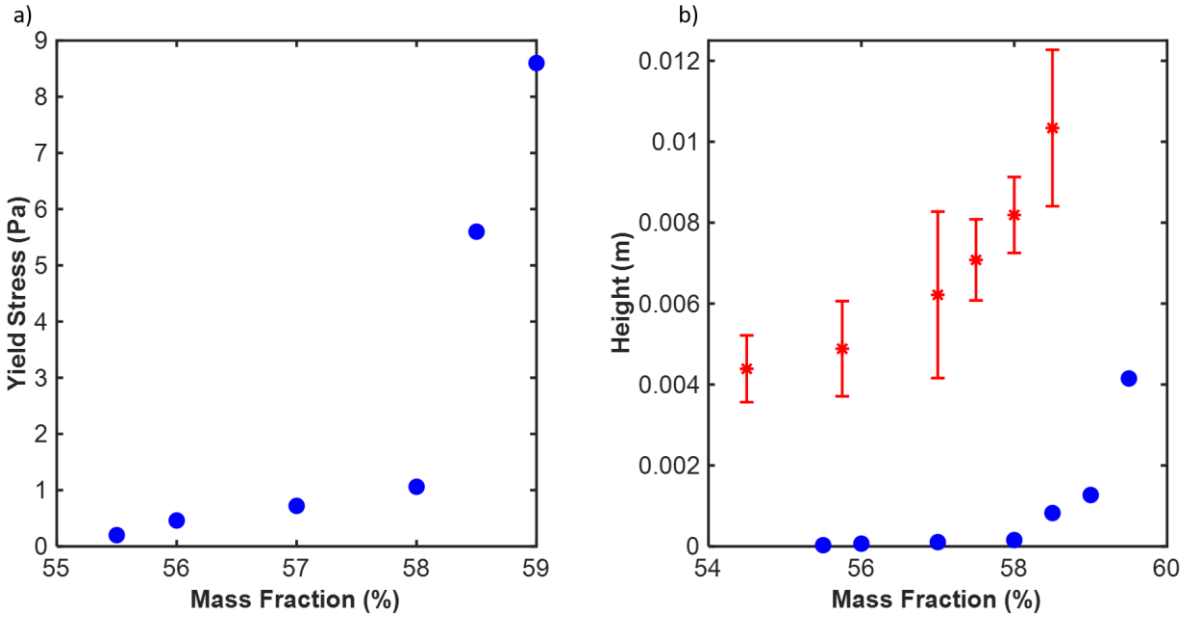

Figure 13: Comparison between the experimentally determined side profile height at τ_2 and a simple model for the height from the rheology determined yield stress. a) yield stress determined from rheology in the relevant range of ϕ_m. b) height estimated from the yield stress using equation (5) (blue) and measured side profile height (red).

The measured side profile height and the estimated side profile height from rheology data have a similar dependence on the cornstarch concentration, but they are considerably far apart in value. Part of this could be due to a time constant, like τ_2, representing 63% of the decay so the drop could continue to thin over time. This small thinning, however, would unlikely account for the large difference. The difference indicates that while the equation (6) captures how the height changes with ϕ_m, other contributions from surface tension or friction might be important as well. Additionally, equation (6) assumes a homogeneous stress field and that the normal yield stress and the shear yield stress are equal. We expect the shear and normal yield stress to scale but not be numerically identical. The similarity between the two data sets suggests that yield stress, while not the only factor, plays a role in determining the relaxed state of the drop. It will be interesting to explore what other properties affect the side profile height to gain a better understanding of that the control parameters governing the relaxation of a dense suspensions.

While creating the rescaling for Figure 10, we noticed that the height at τ_2 and τ_2 itself have an uncannily analogous dependence on the cornstarch concentration, as shown in Fig. 14; the two data sets superimpose almost perfectly, except for ϕ_m =54.5% likely due to similar reasons as mentioned before.

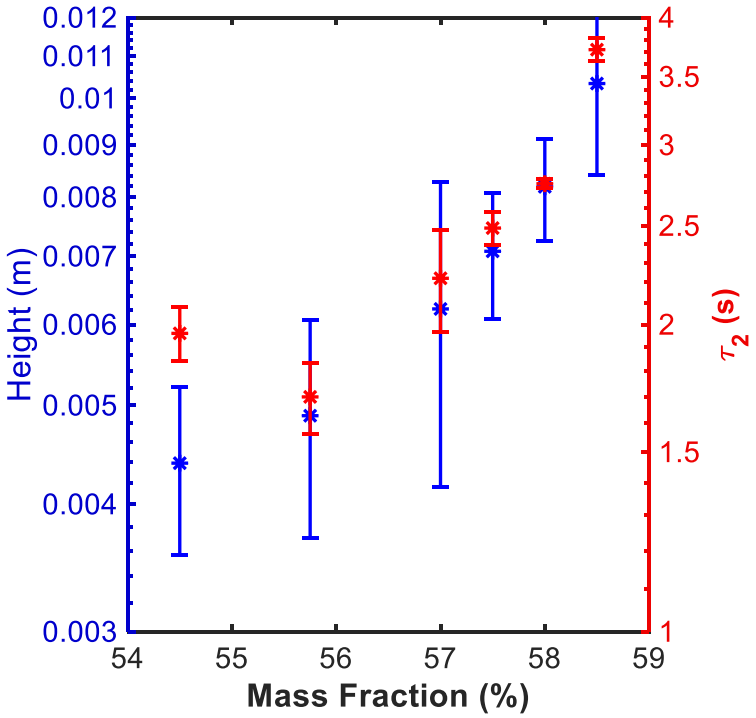

Figure 14: The side profile height at τ_2 (blue) and τ_2 exhibit a similar dependence on the cornstarch concentration.

We hypothesize that the similar functional form results from both parameters being related through the yield stress, which halts the spread of the sample and determines the properties characterizing the final state of our experiment.

4. Conclusions

We show that dense suspensions exhibit a double exponential relaxation characterized by two distinct timescales. The shorter timescale, τ_1, is independent of the cornstarch concentration ϕ_m and denotes the settling of the drop onto the flat surface. The longer timescale, τ_2, increases as ϕ_m increases above 55.75% and is governed by the viscosity of the drop. The drop of dense suspension continues to spread until the gravitational forces driving the spreading are balanced by the yield stress of the suspension.

Future studies could expand on this data by exploring the relationship between the side profile height and the second timescale of the relaxation. Understanding this relationship would further unlock the exact mechanisms that govern dense suspension relaxation. Additionally, to expand on the results a similar experiment could be performed on other dense suspensions to determine if the double exponential behavior is general to all dense suspensions.

Acknowledgments

The author would like to thank Dr. Bischofberger and Jae Hyung Cho for their guidance and assistance throughout the study. Additionally, he would like to thank Dr. Peters for his advice during the study.

References

[1] Baumgarten, A. S. & Kamrin, K. A general constitutive model for dense, fine-particle suspensions validated in many geometries. *Proc Natl Acad Sci USA* **116**, 20828–20836 (2019).

[2] Peters, I. R., Majumdar, S. & Jaeger, H. M. Direct observation of dynamic shear jamming in dense suspensions. *Nature* **532**, 214–217 (2016).

[3] Wyart, M. & Cates, M. E. Discontinuous Shear Thickening without Inertia in Dense Non-Brownian Suspensions. *Phys. Rev. Lett.* **112**, 098302 (2014).

[4] Boyer, F., Sandoval-Nava, E., Snoeijer, J. H., Dijksman, J. F. & Lohse, D. Drop impact of shear thickening liquids. *Phys. Rev. Fluids* **1**, 013901 (2016).
[5] Morris, J. F. Shear Thickening of Concentrated Suspensions: Recent Developments and Relation to Other Phenomena. *Annu. Rev. Fluid Mech.* **52**, 121–144 (2020).
[6] Mari, R., Seto, R., Morris, J. F. & Denn, M. M. Shear thickening, frictionless and frictional rheologies in non-Brownian suspensions. *Journal of Rheology* **58**, 1693–1724 (2014).
[7] Lee, Y. S., Wetzel, E. D. & Wagner, N. J. The ballistic impact characteristics of Kevlar® woven fabrics impregnated with a colloidal shear thickening fluid. *Journal of Materials Science* **38**, 2825–2833 (2003).